An Automatic integrated image segmentation, registration and change detection method for water-body extraction using HSR images and GIS data

Haigang Sui [a,*], Guang Chen [a], Li Hua [b]

[a] State Key Laboratory of Information Engineering in Surveying, Mapping and Remote Sensing, Wuhan University,
430079 Wuhan, China - haigang_sui@263.net
[b] College of resources and environment, Huazhong Agricultural University, 430070 Wuhan, China -
huali@mail.hzau.edu.cn

KEYWORDS: water-body extraction, image segmentation, registration, change detection, GIS;

ABSTRACT:

Automatic water-body extraction from remote sense images is a challenging problem. Using GIS data to update and extract water-body is an old but active topic. However, automatic registration and change detection of the two data sets often presents difficulties. In this paper, a novel automatic water-body extraction method is proposed. The core idea is to integrate image segmentation, image registration and change detection with GIS data as a whole processing. A new iterative segmentation and registration strategy is proposed. Here, the so-called visual attention model and level set segmentation algorithm is introduced to find interesting areas with suspected water-bodies and to obtain initial objects contours. And an improved shape curve similarity (ISCS) is presented to match image segmentation objects and GIS water-bodies with overall spatial constraints. Furthermore buffer based change detection algorithm is designed to obtain unchanged water-bodies and SVM classifier is used to verify changed ones. Experiment results show that proposed method was effective in rapid extraction and change detection of water-bodies.

1. INTRODUCTION

Water resources which have close relationship with daily life play an important role in natural disaster (Barton and Bathols, 1989), environmental (Ke, 2004), transportation and region planning, agricultural production and so on. The observation of water resources using remote sensing images is extensive in recent years for its generalization and effectiveness (Wang and Ma, 2009). The availability of high spatial resolution (HSR) images makes it possible to precisely locate and identify water-body. However it brings new challenges to traditional information extraction techniques. It is generally agreed that water-body holds different radiometric characteristics between images taken within different time and space while the diversity is more prominent in HSR images. In addition, HSR images provide more ground details which make it difficult to extract objects exactly especially with disturbance of noise. The last, even if extraction of water-bodies is well performed, registration and change detection are also hard works because of seasonally change of water-bodies.

Nowadays, many approaches have been developed to deal with the extraction of water-body from HSR images. Typical methods of water-body extraction are mainly based segmentation and classification, such as multi-stage threshold segmentation (Luo et al., 2009), knowledge-based decision-tree classification (Chen et al., 2013) and so on. Some of them can give better results with experimental data. Recently many kinds of water index such as NDWI (Gao, 1996), MNDWI (Xu, 2006) and NWI (Ding, 2009) have been propose and developed. Some indexes have been proved to be effective for indication of water-body presence in HSR images especially for those images with near-infrared or middle-infrared bands (Wang and Ma, 2009). However, automatic extraction is far from achieved. It can be addressed as the follow aspects: 1) A lot of algorithms depend on the manual determination of thresholds based on experiences, and the parameter can't self-adjust adaptively while dealing with various images 2) Some methods consider the fusion of multi-source data such as image and GIS data for extracting

water-body, the processing procedure is commonly semi-automatic because the registration of data sets have to be done manually. 3) Change detection is less integrated within extraction processing. Obviously, automatic approaches considering multi-source data are required with the real-time application requirements such as disaster response emergency situations.

Aiming at the above problems, a novel automatic water-body extraction method is proposed. The core idea is to integrate image segmentation, image registration and change detection with GIS data as a whole processing. To achieve the purpose, the following strategies are employed.

1) Iterative segmentation is designed to avoid manual adjustment of parameters. The CV model of level-set method is used to segment features of HSR image iteratively. Model parameters are adjusted adaptively by input the last segmentation results as initial contours.

2) Segmentation and matching are integrated to achieve automatic registration between image and GIS data. Iterative strategy reduces the importance of segmentation model and meanwhile, enhances the adaptiveness of segmenting process. Improved shape curve similarity (ISCS) are proposed as similarity measures of image segmentation objects and GIS water-bodies which provide stable shape feature. In the end, matching results are constraints by spatial consistency of control points.

3) Buffer based change detection are carried out to confirm unchanged water-bodies. Then, their features are used to train SVM classifier and to verify suspected water-bodies.

The rest of this paper is organized as follows. Section II describes the proposed method. Section III analyses and compares the experimental results, followed by the conclusion in Section IV.

2. METHODOLOGY

The framework of proposed method is shown in Figure.1. It consists of three blocks: first, saliency-based

visual attention model (Itti et al., 1998) is employed to detect water-bodies and OTSU algorithm (Otsu, 1979) is used to obtain an adaptive threshold for segmentation to get the initial extraction results (see Section 2-A); 2) level-set evolution and shape similarity based registration are carried out iteratively to optimize evolution and registration results (see Section 2-B); 3) SVM is trained by texture features of matched segmentation objects and it is used to validate unmatched objects for change detection (see Section 2-C).
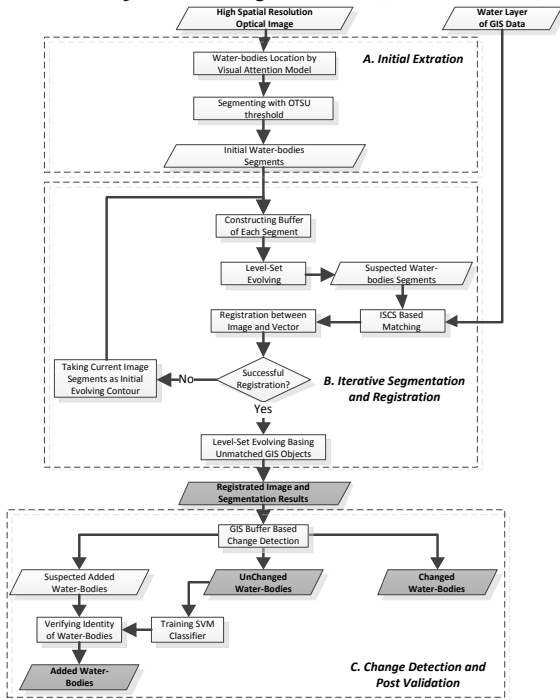

Figure.1 Framework of the proposed method

A.   Segmentation of Suspected Water-bodies Based on Visual Attention Model

Water-bodies always show different spectral response in high spatial resolution optical (HSRO) images due to pollution, sediment or other factors. So the traditional methods of using a global model/scale for extracting whole water-bodies will fail to cover the detail of water-body. Considering the significance of water-body, a multi-scale saliency-based visual attention model is employed to detect water-bodies in HSRO images. Then threshold segmentation is executed on sub images detected by visual attention with threshold obtained by OTSU algorithm.

Saliency-based visual attention model was inspired by the behaviour and neuronal architecture of the early primate visual system (Itti et al., 1998). This model represents a complete account of bottom-up saliency and does not require any top-down guidance to shift attention. There are three main stages to initial model and detect salient targets.

1) Feature maps' computation. Input image is first decomposed into a set of topographic feature maps by scales, colours, intensity, orientations.

2) Salient map generation. Different spatial locations then compete for saliency within each map, such that only locations which locally stand out from their surround can persist. All feature maps feed, in a purely bottom-up manner, into a master "saliency map," which topographically codes for local conspicuity over the entire visual scene.

3) Focus of attention (FOA) shift. Active locations on salient map compete with each other and the winner will be the next FOA.

A set of salient sub images which containing water-body will be obtained by visual attention. The sub images are segmented respectively with thresholds obtained by OTSU algorithm which keeping maximum class variance in each sub images. Class variance represent difference of pixel value between foreground and background which obtained by threshold segmentation.

$$g = w_0 w_1 (\mu_0 - \mu_1)^2 \qquad (1)$$

where g represent class variance, w_0 indicate proportion of foreground pixel number, μ_0 indicate average pixel value of foreground pixel, w_1 indicate proportion of background pixel number, μ_1 indicate average pixel value of background pixel.

B.   Iterative Image Segmentation and Registration

The rough outlines of water-bodies in HSRO image are obtained in initial extraction. Aiming at approaching outlines of water-bodies to the real boundary, level-set method was employed in image segmentation. In this paper, the multi-scale level set approach (Sui et al., 2012) was used for segmenting features in HSRO image to overcome the problems of large data volumes and noise in images. Initial extraction results are taken as the initial contour of level set model.

Let u be an input image, and C be a curve in the image domain Ω. According to (Chan and Vese, 2001), segmentation is performed by evolving such that it minimizes the energy functional below:

$$E(\emptyset, \ u_1, \ u_2) = $$
$$\alpha_1 \int_\Omega (u - u_1)^2 H(\emptyset) dx dy + \alpha_2 \int_\Omega (u - u_2)^2 (1 - H(\emptyset)) dx dy + \beta \int_\Omega H(\emptyset) dx dy + \gamma \int_\Omega \delta(\emptyset) |\nabla \emptyset| dx dy \qquad (2)$$

where constants u_1, u_2 are the averages of pixel value of input image u inside C and outside C , respectively, and $\alpha_1, \alpha_2, \beta, \gamma$ are non-negative weighted parameters. Function $\emptyset(x, y)$ represents class Ω_1 for $\emptyset(x, y) > 0$, and class Ω_2 for $\emptyset(x, y) < 0$. The Heaviside function $H(\emptyset)$ and one-dimensional Dirac function $\delta(\emptyset)$ are introduced to simplify the energy function.

$$H(\emptyset) = \begin{cases} 1, & \emptyset \geq 0 \\ 0, & \emptyset < 0 \end{cases}, \quad \delta(\emptyset) = \frac{d}{d\emptyset} H(\emptyset) \qquad (3)$$

The evolution of $\emptyset$ is governed by the following motion partial differential equation to minimize energy functional E.

$$\frac{\partial \emptyset}{\partial t} = \delta(\emptyset) \left[\gamma \nabla \cdot \left(\frac{\nabla \emptyset}{|\nabla \emptyset|} \right) - \alpha_1 (u - u_1)^2 + \alpha_2 (u - u_2)^2 - \beta \right] \qquad (4)$$

Vector set V_{img} was obtained by vectorizing (Zhang et al., 2008) binary image generated by segmenting input HSRO image with level-set method. Improved shape curve similarity (ISCS) based registration was employed between V_{img} and V_{gis} contained in water layer of existing GIS data. Shape curve is proposed in (Chen et al., 2006) as a method of shape representation. In other words, shape curve is a marking diagram generated by angle-distance pattern whereas the corresponding may be ambiguous with concave polygon. Aiming at the problem, our improving focuses on generation of marking diagram that distance-distance pattern is proposed. Instead of sampling at fixed angle interval, points are picked up at distance interval of P/n where n denote the sampling number and P represent perimeter of

polygon. Test results are shown in Figure.2. To avoid the dependence on scale, distances are normalized basing on formula (5).

$$d(i) = \frac{d_i(i)}{d_{max}}, i = 1 \dots n \qquad (5)$$

where $d_i(i)$ denote distance between the i-th sampling point and centroid of polygon, d_{max} represent the max value of all distances.
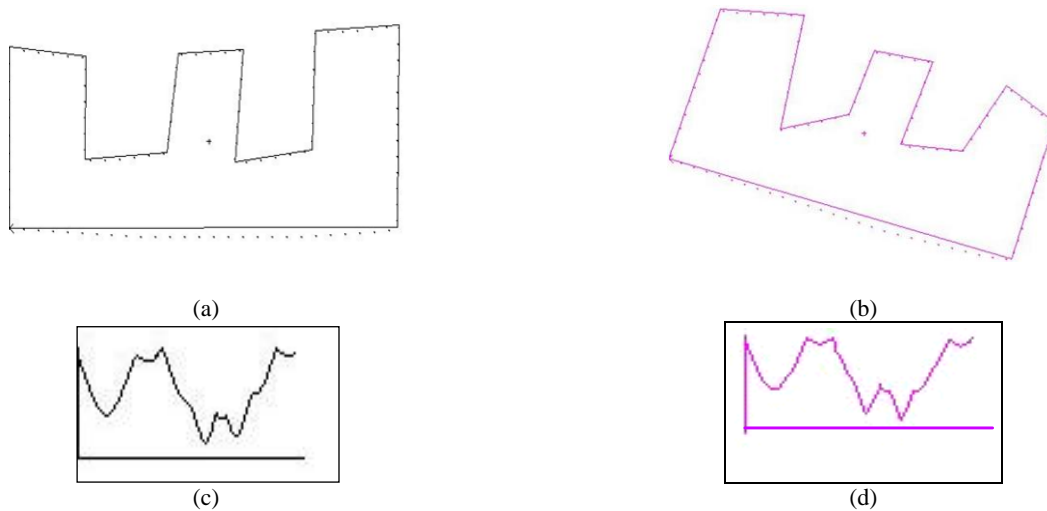
ISCS is obtained basing on calculating correlation between sets of sampling points by equation (6). The starting point index of polygon to be matched has to be shift gradually that to obtain the best matching position.

(a)

(b)

(c)

(d)

Figure.2 Polygons and corresponding shape curves. (a) polygon A. (b) polygon B. (c) shape curve of polygon A. (d) shape curve of polygon B that have been shift to the satisfied matching position.

$$pCor\_shape(A, B) = \max\left(\frac{\sum_{k=1}^{n_p}(d_k^A - \overline{d^A})(d_{1k}^B - \overline{d_1^B})}{\sqrt{\sum_{k=1}^{n_p}(d_k^A - \overline{d^A})^2 \sum_{k=1}^{n_p}(d_{1k}^B - \overline{d_1^B})^2}}\right), l = 1,2\dots n_p \quad (6)$$

Aiming at the case that multi-similar objects exist, the final matching results have to consider the constraint of spatial. Geometric transformation equation (7) is solved with the initial matching sets of points.

$$\begin{cases} x_v = a_0 + a_1 \times x_r + a_2 \times y_r \\ y_v = b_0 + b_1 \times x_r + b_2 \times y_r \end{cases} (7)$$

Where x_v, y_v represent coordinates of each selected objects from V_{gis}, x_r, y_r represent coordinates of each selected objects from V_{img}.

The coordinates of centroid of all the objects in V_{img} are transformed according to equation (7). If one centroid of object in V_{gis} fall within the circle with the centre of one transformed centroid and the radius of D_{buf}, the two centroids are considered as one pair of matched points. The proportion of centroids number of matched (PCM) in V_{gis} is taken as an indicator that whether registration is success. When PCM is greater than threshold T_{pcm}, the registration is success, and vice versa.

The accurate of level-set segmentation results is the main reason for failure registration. The scheme of iterative segmentation and registration with current V_{img} as initial contour of level-set method is employed and the iteration would not stop until successful registration.

C. Buffer Based Change Detection and SVM Verifying

Considering the fact that water-bodies' changes are moderate during short time, water data of GIS was taken as priori knowledge to identify unchanged water-bodies. Buffer

based change detection (Dong et al., 2009) (Sui, 2002) were performed between V_{img} and GIS data. As a result, V_{img} were divided into unchanged ones and changed ones that the former were identified as water-bodies and the latter were suspected water-bodies which had to be verified. Features of confirmed water-bodies and background were extracted to train the SVM classifier (Burges, 1998) which was employed in verifying suspected water-bodies. Eigenvectors were constructed by spectrum and texture which were extracted by Gabor filter (Tai, 1996). Sample selection scheme and feature extraction method were describe in three parts.

1) Sliding a N × N sub window within the bounding rectangle of confirmed water-bodies with step of N in X and Y directions. The positive samples are selected while the sub window fall in water-bodies' area. The negative samples are selected from input image except the areas of V_{img} in the same way.

2) Calculating pixel mean value of samples in three bands and obtaining a 3-dimensional features vector. Texture features were obtained by Gabor filter (Han and Lin, 2008) in eight directions, then mean and variance of Coefficient magnitude sequence would be obtained in one direction. As a result, a 19-demensional vector containing spectrum and texture features would be obtained from one sample. More details about texture features extraction can be seen in (Han and Lin, 2008).

3) Sampling the suspected water-bodies in V_{img} with method described in step 1 and Extracting features as description in step 2. Then samples were verified by SVM classifier and authenticated samples were confirmed water-bodies which had changed.

3. EXPERIMENTAL RESULTS

A. WorldView-II/1:10000 Electronic map data

This experiment was conducted on a WorldView-II image with three visible bands of 0.5-m spatial resolution and electronic map data with scale of 1:10000 over the suburbs of Hangzhou, China. The experiment data and results are shown in Figure.3 (a) to (d).
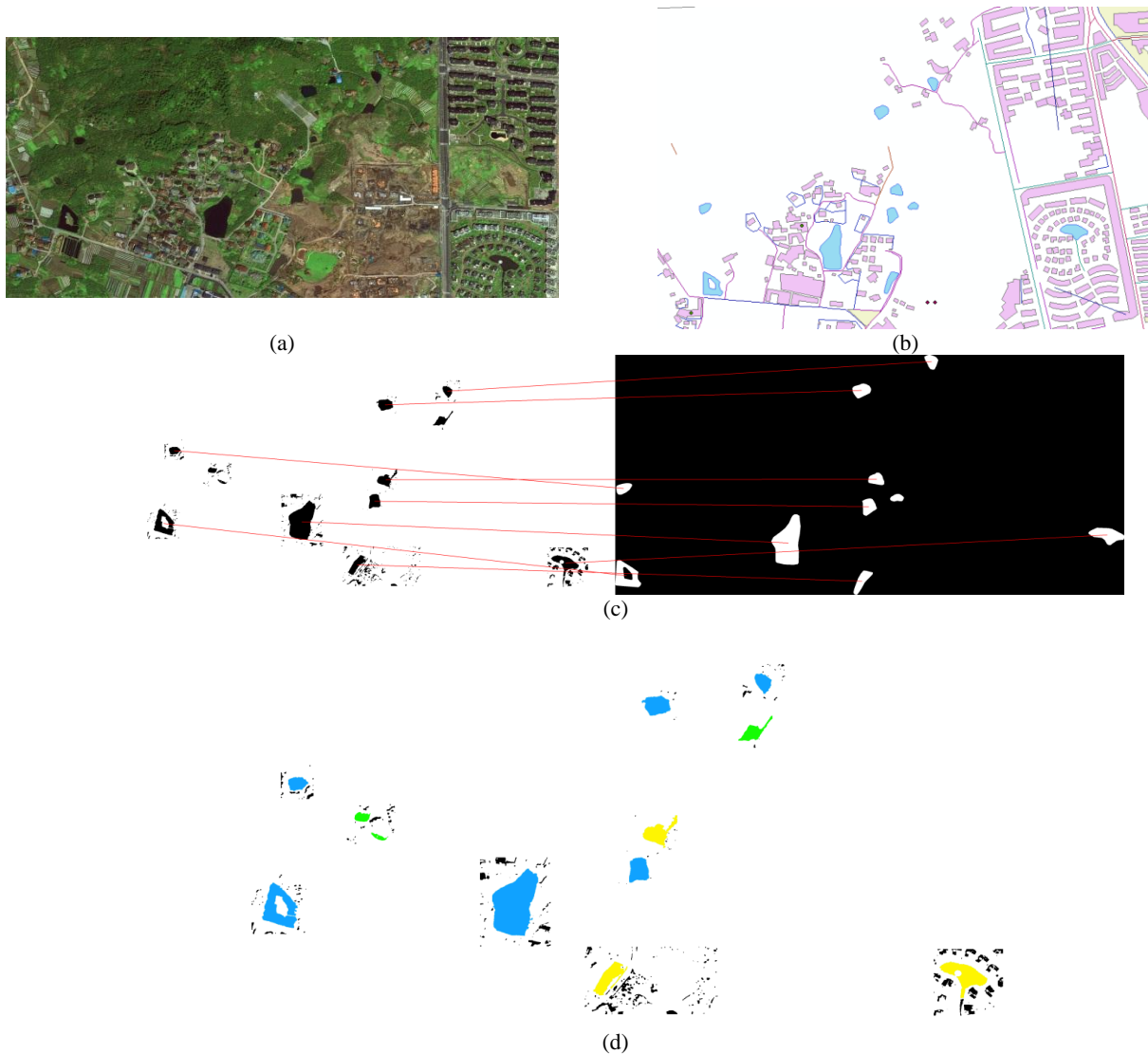

(a)

(b)

(c)

(d)

Figure.3 Registration and water-body extraction result of data set A. (a) optical image. (b) 1:10000 GIS data over the same area of image. (blue objects represent data of water layer) (c) Registration results (left is initial extraction results; right is GIS data of water-bodies; red lines represent matching relations). (d) final water extraction result (blue objects represent unchanged water-bodies, yellow objects represent changed ones and green objects represent newly added water-bodies)

B. WorldView-II /OpenStreetMap

The second data set consist of WorldView-II image with three visible bands of 0.5-m spatial resolution and OpenStreetMap (OSM) data which corresponds to the area of Beijing, China. The experiment area cover a wider range than data set A and it is urban area consisted of buildings, roads, vegetation, open areas and water-bodies. The experiment data and results are shown in Figure.4 (a) to (d).
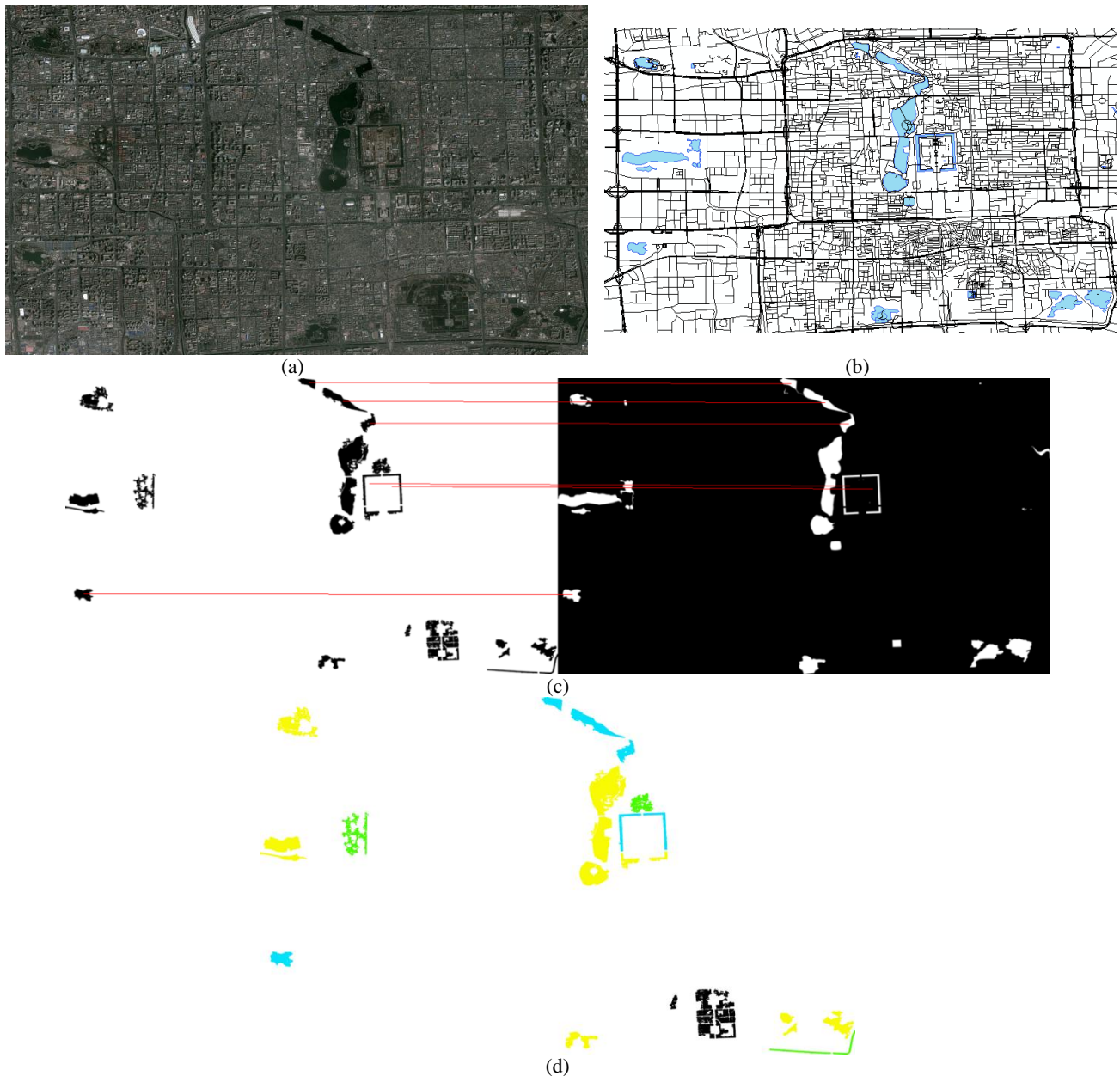
Figure.4 Registration and water-body extraction result of data set B. (a) optical image. (b) OSM data. (blue objects represent data of water layer) (c) Registration results (left is initial extraction results; right is GIS data of water-bodies; red lines represent matching relations). (d) final water extraction result (blue objects represent unchanged water-bodies, yellow objects represent changed ones and green objects represent newly added water-bodies)

Registration image and water-body extraction results were two main production of our proposed method. Therefore we evaluated proposed method by calculating the accuracy of registration and extraction respectively. The accuracy of registration is evaluated using the root mean squared error (RMSE). Due to less control points, we obtain other 20 matching points manually to increase the reliability of RMSE. The calculation results from experiment A and B are 4.69 and 5.07. These quantitative results don't show advantage compared with images registration results of traditional method. However, cartographic generalization and scale factor impact on feature matching seriously. What more, unlike image, GIS data include only specific feature emit its distribution is discrete, so that RMSE represent the registration accuracy of water areas where we focus on and it is sufficient for demand of change detection.

The main types of water-bodies in experiment data are pools and miniature lakes which discretely distribute in the experiment area. These water-bodies have stable and unique shape features. In experiment A, there are 9 pairs of control points obtained from experiment data that include most water-bodies of GIS. In some case, vegetation beside water-body is segmented as part of water for they have similar spectrum. It will affect water-bodies' shape and cause failure matching. On the other hand, cartographic generalization is carried out with small-scale GIS which also modify form of water-bodies. It is for above reasons that only 6 pairs of control points are obtained.

Centroids of matched water-bodies are taken as control points, therefore its distribution are related to the distribution of water-bodies. In experiment, control points are not well-distributed, whereas the registration accuracy of water area is sufficient.

Water-body extraction results are consisted of unchanged, changed and newly added water-bodies. Quantitative statistics of the results are compared in Table 1, where omission errors (OE) and commission errors (CE) are used to evaluate the accuracy of water-bodies detection.

Compared with ground truth, water-bodies of unchanged and changed are obtained without missing. However, extraction of newly added water-bodies is not totally successful that omission extraction and wrong extraction occur. The quantitative results shown in Table 1 represent that extraction accuracy decline from that of unchanged ones to that of newly added ones. This trend explain that extraction accuracy have positive correlation with variety of water-bodies. As for the overall accuracy, it is acceptable that less than 25%. Analysis shows the following reasons that cause extraction error. First, these errors may come from registration error and effect of uncertainty of water-body's boundary because of shelter nearby. Furthermore, error of newly added water-bodies is higher, due to omission extraction of some tiny water-bodies which are not salient in specified scale. The last, in some garden area, such as experiment B, water-bodies with complex contour are overlapping with plants that are hard to distinguish and cause wrong extraction.

Table 1   Water-Body extraction accuracy of proposed method

Data Set	Items	Accuracies	
		OE (%)	CE (%)
WorldView-2/ 1:10000 Electronic map data	Unchanged	5.05	13.25
	Changed	17.41	13.25
	Newly Added	20.01	21.19
WorldView-II / OpenStreetMap	Unchanged	4.88	6.99
	Changed	11.82	19.68
	Newly Added	14.02	24.15

4. CONCLUSIONS

In this study, a water-body extraction framework is proposed based on integrated image segmentation, registration and change detection. GIS data are co-processed with images to improve extraction results. It should be noted that some issues have to be paid more attention. First, processing with seasonal rivers may encounter problem that it will miss extraction in winter when the river drying. Additionally, processing on newly added water-bodies have to be paid more attention that some of them are not salient enough to be detected or confused with background.

5. ACKNOWLEDGEMENT

REFERENCES

Barton, I.J. and Bathols, J.M., 1989. Monitoring floods with AVHRR. Remote Sensing of Environment, 30(1): 89-94.

Burges, C.J.C., 1998. A Tutorial on Support Vector Machines for Pattern Recognition. Data Mining and Knowledge Discovery, 2(2): 121-167.

Chan, T.F. and Vese, L.A., 2001. Active contours without edges. Image Processing, IEEE Transactions on, 10(2): 266-277.

Chen, J., Liu, S., Wang, C., You, S. and Wang, Z., 2013. Research on Urban Water Body Extraction Using Knowledge-based Decision Tree. Remote Sensing Information, 28(1): 29-33,37.

Chen, X., Ye, M. and Ni, C., 2006. A Method for Shape Recognition. PATTERN RECOGNITION AND ARTIFICIAL INTELLIGENCE, 19(6): 758-763.

Ding, F., 2009. Study on information extraction of water body with a new water index (NWI). SCIENCE OF SURVEYING AND MAPPING, 34(4): 155-157.

Dong, M., Zhang, H., Zhu, X. and Chen, C., 2009. Change Detection of Road Networks Based on Remote Sensing Image. Geomatics and Information Science of Wuhan University(02): 178-182.

Gao, B., 1996. NDWI—A normalized difference water index for remote sensing of vegetation liquid water from space. Remote Sensing of Environment, 58(3): 257-266.

Han, M. and Lin, X., 2008. CLASSIFICATION ALGROITHM OF REMOTE SENSING IMAGE BASED ON WEDGELET TRANSFORM. Journal of Infrared and Millimeter Waves(04): 280-284.

Itti, L., Koch, C. and Niebur, E., 1998. A model of saliency-based visual attention for rapid scene analysis. Pattern Analysis and Machine Intelligence, IEEE Transactions on, 20(11): 1254-1259.

Ke, C., 2004. A REVIEW OF MONITORING LAKE ENVIRONMENT CHANGE BY MEANS OF REMOTE SENSING. TRANSACTIONS OF OCEANOLOGY AND LIMNOLOGY(4): 81-86.

Luo, J., Sheng, Y., Shen, Z., Li, J. and Gao, L., 2009. Automatic and high-precise extraction for water information from multispectral images with the step-by-step iterative transformation mechanism. JOURNAL OF REMOTE SENSING, 13(4): 604-615.

Otsu, N., 1979. A Threshold Selection Method from Gray-Level Histograms. Systems, Man and Cybernetics, IEEE Transactions on, 9(1): 62-66.

Sui, H., 2002. Automatic change detection for road networks based on features. Dissertation Thesis, WuHan University.

Sui, H., Xu, C., Liu, J., Sun, K. and Wen, C., 2012. A novel multi-scale level set method for SAR image segmentation based on a statistical model. International Journal of Remote Sensing, 33(17): 5600-5614.

Tai, S.L., 1996. Image representation using 2D Gabor wavelets. Pattern Analysis and Machine Intelligence, IEEE Transactions on, 18(10): 959-971.

Wang, H. and Ma, M., 2009. A Review of Monitoring Change in Lake Water Areas Based on Remote Sensing. REMOTE SENSING TECHNOLOGY AND APPLICATION, 24(5): 674-684.

Xu, H., 2006. Modification of normalised difference water index (NDWI) to enhance open water features in remotely sensed imagery. International Journal of Remote Sensing, 27(14): 3025-3033.

Zhang, X., Wang, M. and Jiang, S., 2008. A Novel Approach for Raster Data Vectorization. Geo-Information Science(06): 6730-6735.